Chapter 5

Mechanical Residual Stresses

5.1 Onset of Iso-Thermal Mechanical Residual Stresses

In grinding, material is removed by mechanical cutting. Although heating and possibly associated phase transformation may change the properties of the workpiece material, iso-thermal mechanical cutting and the induced residual stresses need to be understood before the mechanisms of residual stresses with a full coupling of all the causes can be explored.

To initiate the iso-thermal plastic deformation in a grinding process, the level of effective stress at a point should be beyond the initial yield stress of the workmaterial. As the grinding stresses rely on the complex nature of the contact mechanisms between a grinding wheel and a workpiece, it is important to consider different grinding tractions and their related stresses. Practically, an actual contact area between a grinding wheel and a workpiece is smaller than the apparent one. This is because there are only a number of active cutting grits in contact with the workpiece. Therefore, it is interesting to investigate the role of the ratio of the actual area to the apparent area, η, while studying the grinding stresses. Under a constant discrete pressure distribution as shown in Fig. 5.1, a higher traction intensity is required to initiate plastic deformation if η is higher. Consequently, the sharpness of the active grinding grits has a key role in stress development. In other words, a grinding wheel with sharper grits needs lower cutting forces which is consistent with practical observation. The ratio of the horizontal to vertical grinding forces, μ, named as the 'friction' factor is another dominant factor leading to the onset of plastic deformation. At a larger 'friction' factor, much less grinding forces are needed to initiate plastic deformation. Figure 5 shows that the critical grinding force can be thought of as a power

the critical grinding force associated with plastic deformation in surface grinding can be further

shown in Fig. 5.1c. For this particular analysis, the critical normal force F_n can be expressed as

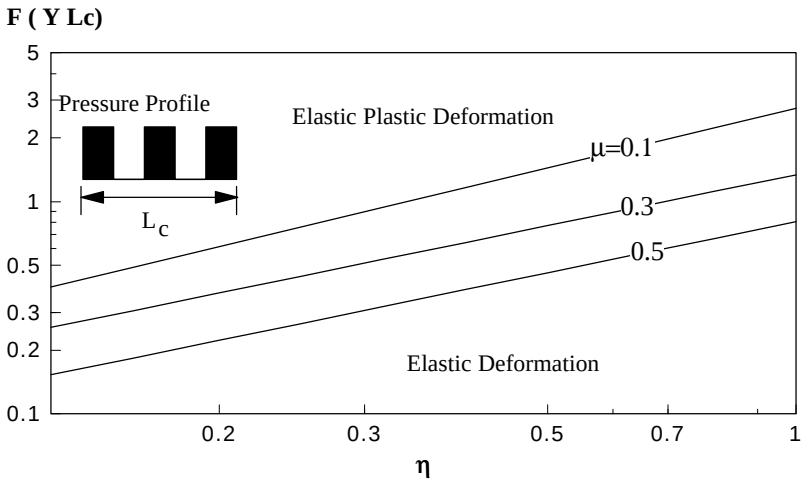

(a) area ratio effect

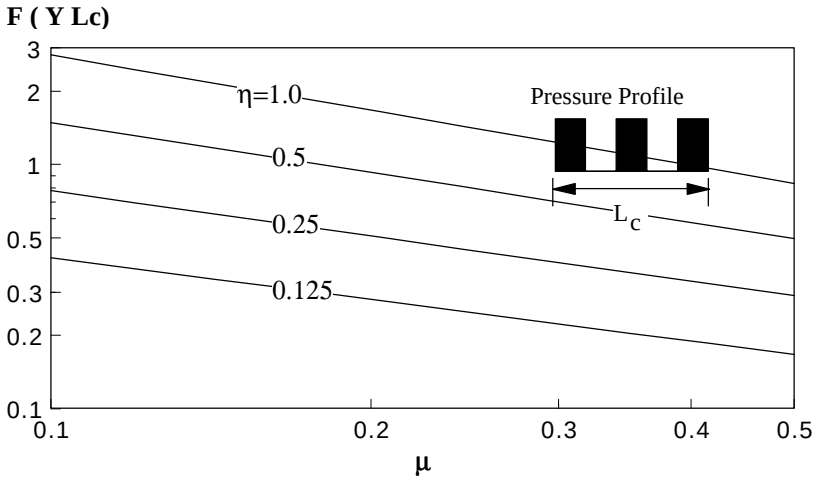

(b) 'friction' factor effect

Figure 5.1 Critical mechanical grinding conditions respect to a constant grinding traction force profile (3 cutting grits)

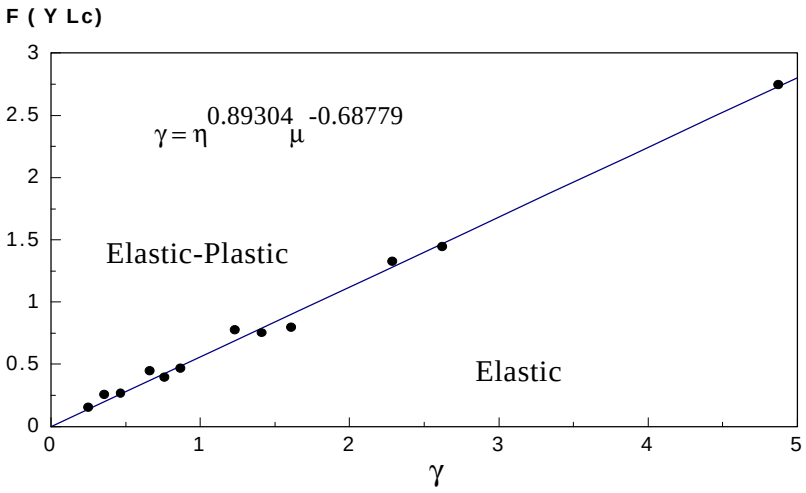

(c) critical force curve

Figure 5.1 Critical mechanical grinding conditions with respect to a constant grinding traction force profile (3 active cutting grits) (continued)

$$F_n = 0.556\, h^{0.89304}\, m^{-0.68779}\, Y\, L_c \qquad 5.1$$

In grinding, the traction on a workpiece surface should be in a triangular profile, as Zhang et al [1993] pointed out. The effect of triangular profiles in relation to the active cutting factor, μ, is shown in Fig. 5.2. The results indicate similar trends as in Fig. 5.1 but with less total grinding force and less effect of the traction in grinding is more critical to the onset of plastic deformation. Moreover, according to Fig. 5.2 the traction associated with an up-grinding mechanism (l_a=0.25) is more critical compared with that of down-grinding ((l_a=0.75). The effect of the active number of cutting grits on the critical grinding force is found to be minor. Thus the effective area ratio is the dominant factor in the initiation of plastic deformation and residual stresses.

To reveal the stress field associated with traction distribution, the iso-effective stresses (von-Mises stress) of the workmaterial prior to yielding are examined in Fig. 5.3. It shows that the maximum effective stresses always near the surface at a distance relying on the friction factor and the traction profile. For an up-grinding process, (l_a=0.25) the maximum effective stress distance from both the ground surface and the leading edge of the traction

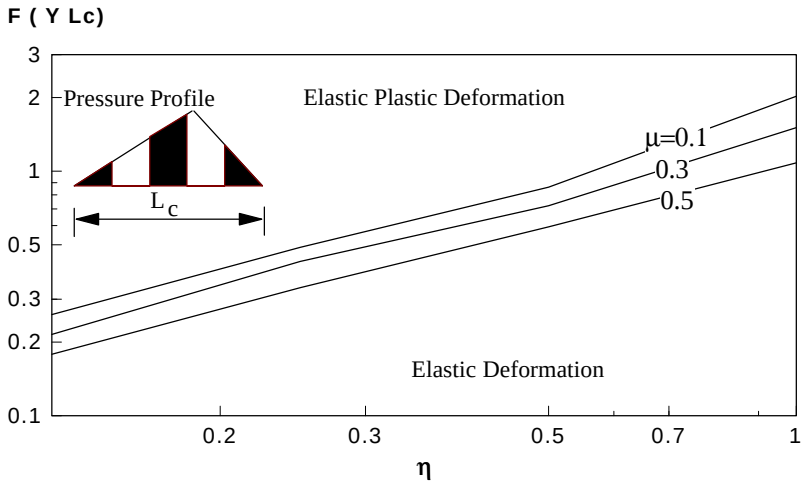

(a) l_a=0.25 (3 active cutting grits)

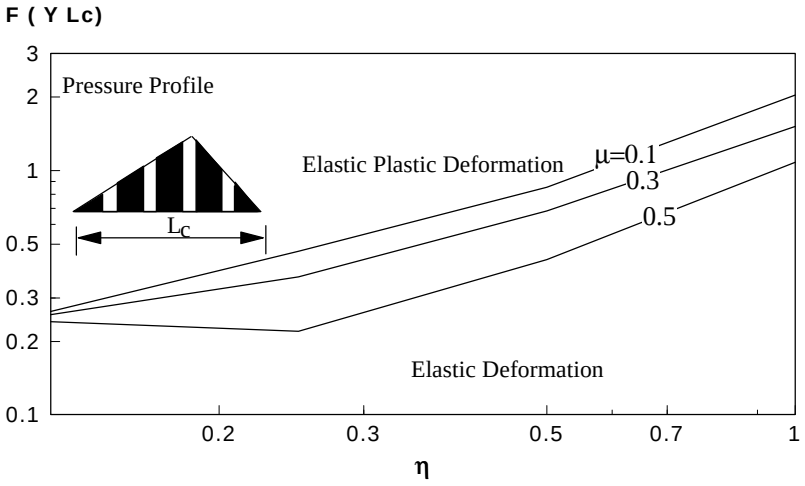

(b) l_a=0.25 (5 active cutting grits)

Figure 5.2 Effects of triangular grinding traction and effective area ratio on the onset of plastic deformation

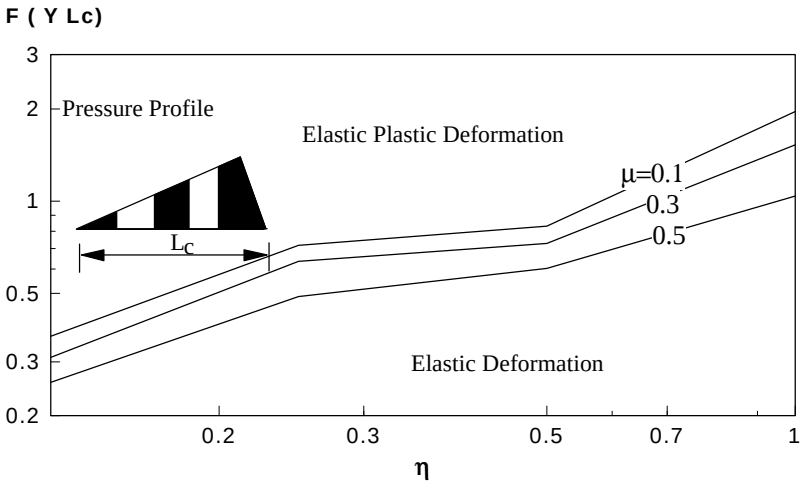

(c) l_a=0.75 (3 active cutting grits)

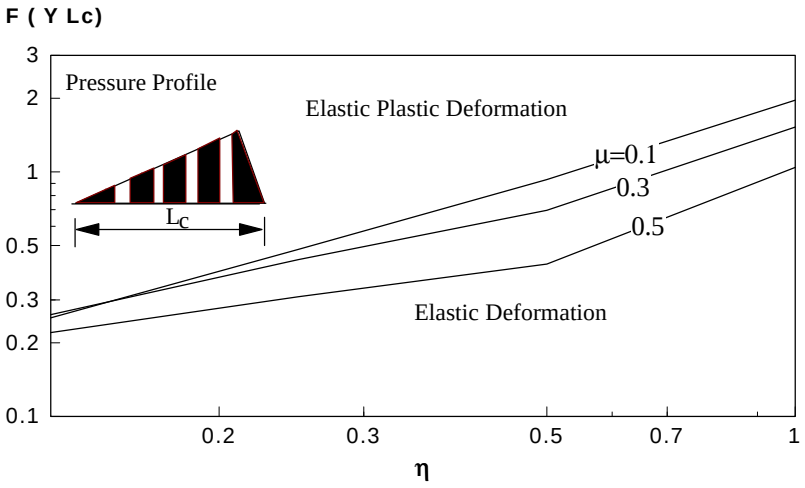

(d) l_a=0.75 (5 active cutting grits)

Figure 5.2 Effects of triangular grinding traction and effective area ratio on the onset of plastic deformation (continued)

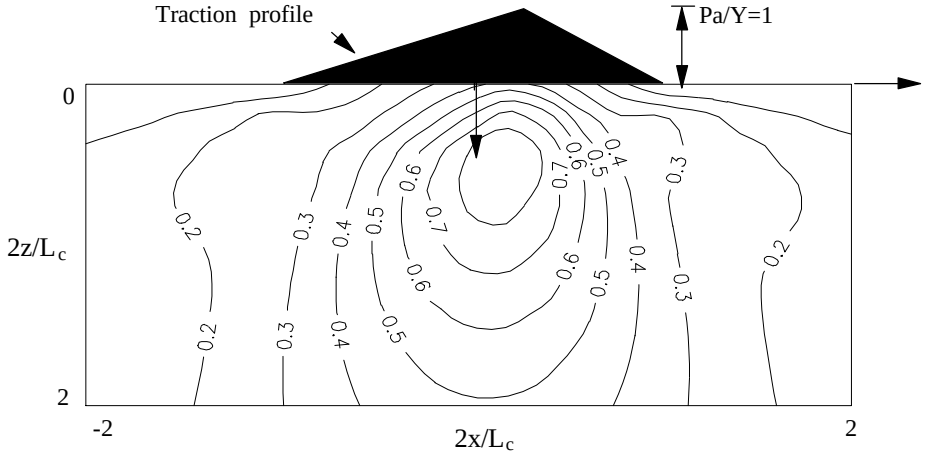

(a) l_a=0.25, μ=0

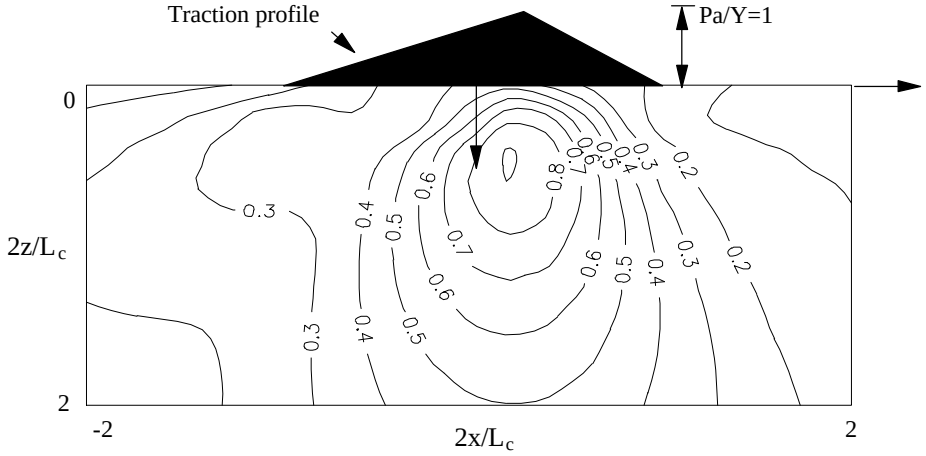

(b) l_a=0.25, μ=0.1

Figure 5.3 Effective stress to yield stress ratio contours

plastic deformation would initiate at a closer distance from both the ground surface and the leading edge of the traction. A down-grinding process has a similar pattern of effective stress contours (Fig. 5.3d) but with a closer distance of maximum effective stress to the grinding surface and the leading edge of traction.

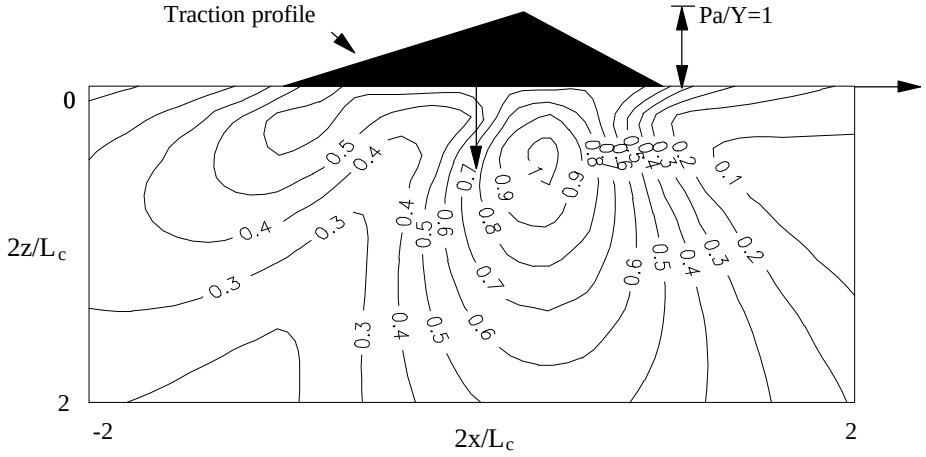

(c) l_a=0.25, μ=0.3

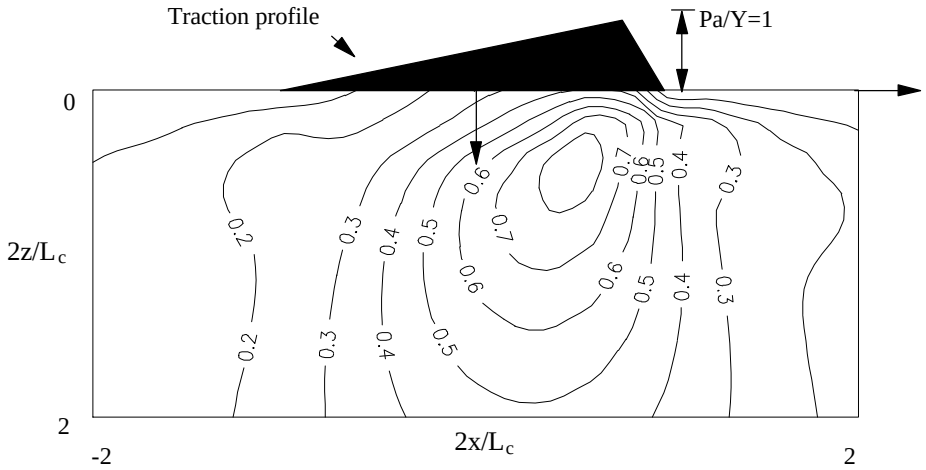

(d) l_a=0.75, μ=0

Figure 5.3 Effective stress to yield stress ratio contours

5.2 Iso-Thermal Grinding Residual Stresses

The first step towards understanding the mechanisms of iso-thermal mechanical residual stresses is to investigate the grinding stress history in terms of grinding conditions. The surface stress history of a typical up-grinding process is shown in Fig. 5.4. It is found that the longitudinal stress, σ_{xx}, starts with compression due to mechanical pressure. As mechanical traction is moving

μ, stretches the ground surface and

gives rise to a tensile residual stress, σ_{xx}. For plane stress, σ_{yy}, compressive stress is developed as traction moves and is not affected by further movements of the load. Thus it is the direction of the horizontal force that determines the nature of longitudinal residual stress, σ_{xx}. It is therefore reasonable to expect that iso-thermal down-grinding processes would result in compressive

As discussed in Chapters 3 and 4, there are two major residual stress components at the workpiece surface, namely, the longitudinal stress along the grinding direction, σ_{xx}, and that perpendicular to the xz-plane, σ_{yy}. Figure 5.5 reveals the roles of the traction profile and the

$\sigma_{xx.}$ With a small

a.

However, the depth of the residual stresses increases from $0.375L_c$ to $0.5L_c$ as traction intensity increases. The same nature of residual stresses is observed.

The compressive nature of the iso-thermal mechanical residual stresses of down-grinding (l_a=0.75) is similar to Ramanath and Shaw (1986) (see Fig. 5.6), although they used CBN wheels. In the present study, the surface compressive stresses in the grinding direction varied linearly, which is also consistent with their result. Another similarity is observed for the decay behaviour of grinding stresses in the subsurface.

residual stresses, $\sigma_{xx.}$ and σ_{yy}, respectively. It is interesting to note that σ_{yy} is mainly

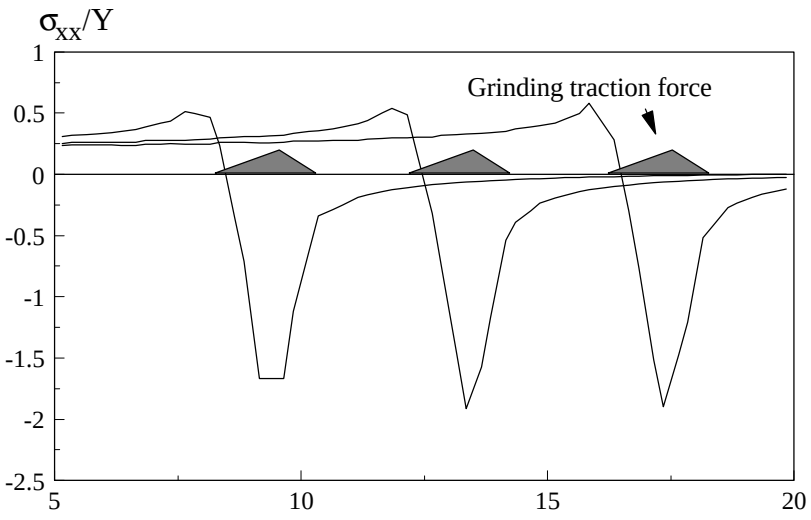

(a) σ_{xx}

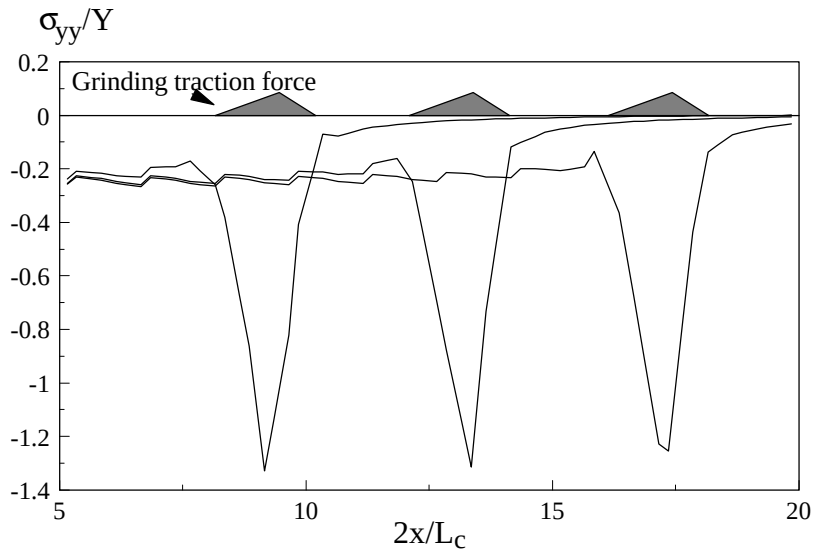

(b) σ_{yy}

Figure 5.4 Mechanical grinding stresses
($p_a/Y=2$, $l_a=0.25$, $\mu=0.3$)

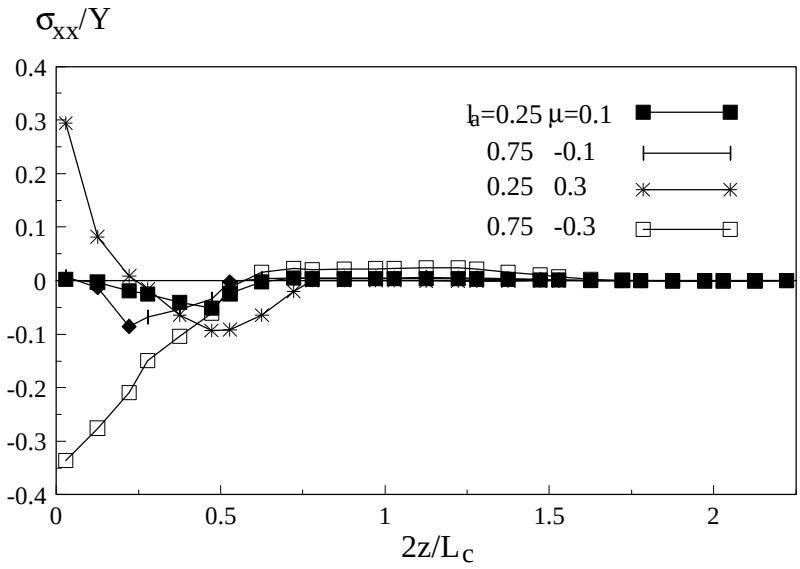

(a) $p_a/Y=2.0$

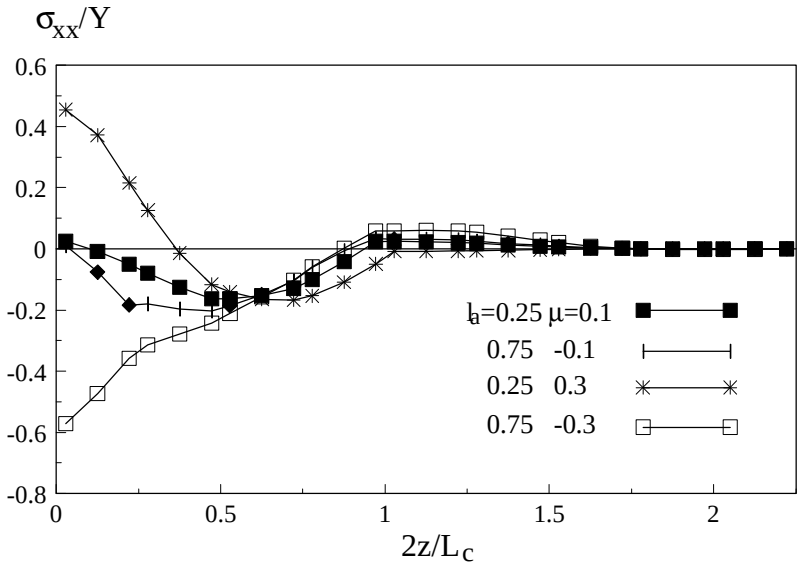

(b) $p_a/Y=2.25$

Figure 5.5 Mechanical grinding residual stresses, 'friction' and grinding mechanisms effect.

compressive, but the nature of σ_{xx} relies largely on the grinding directions and on the magnitude of the 'friction' factor μ. For an up-grinding ($\mu>0$), σ_{xx} is always tensile. However, a down-grinding ($\mu<0$) may yield either compressive or tensile surface residual stresses, μ. Figure 5.7b indicates that a compressive

longitudinal stress σ_{xx} may be achieved if the magnitude of the 'friction' factor is sufficiently large ($|\mu| > 0.2$). Practically this can be done by employing down-grinding and maintaining the ratio of the horizontal to vertical grinding forces above 0.2.

To reveal the plastic zone history in relation to the mechanical load movements across the ground surface, a typical plastic zone development is examined and demonstrated in Fig. 5.8. It shows that a plastic zone is moving together with the mechanical load under steady state grinding conditions.

It should be noted that not only the critical grinding forces but also the distributions and magnitude of residual stresses are sensitive to the profile of moving surface stresses. This is clearly shown in Fig 5.9. The residual stress levels associated with a moving surface traction with a less active effective cutting area are much higher than those with

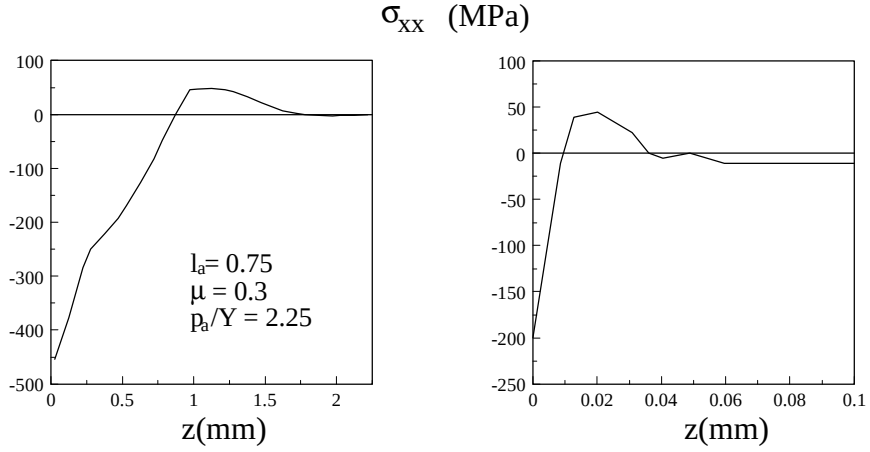

(a) workmaterial EN23 steel, iso-thermal mechanical grinding conditions (present study)

(b) workmaterial case carburised steel, air cooling, CBN wheel, v_{wh} =32m/sec, d_c = 0.012 mm, v = 0.14 m/sec (Ramanath and Shaw (1986))

Figure 5.6 Grinding residual stresses

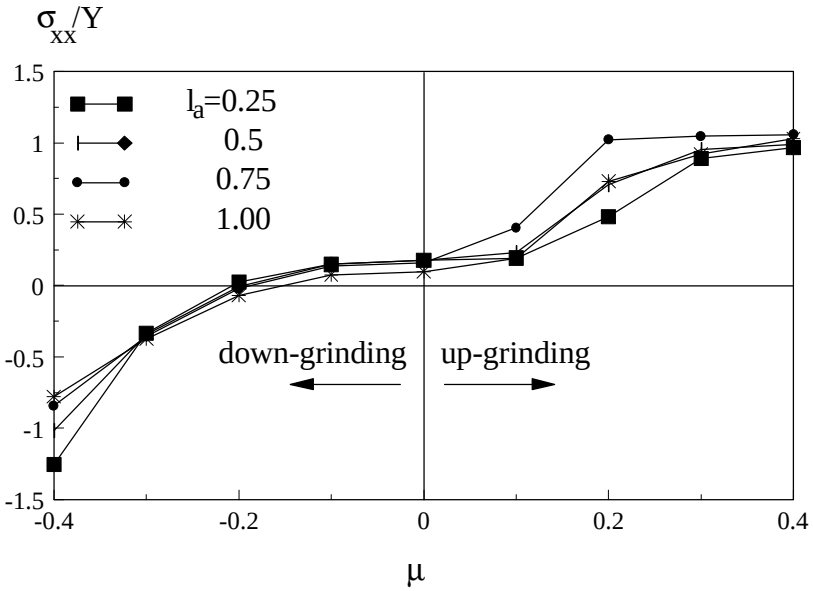

(a) σ_{xx}

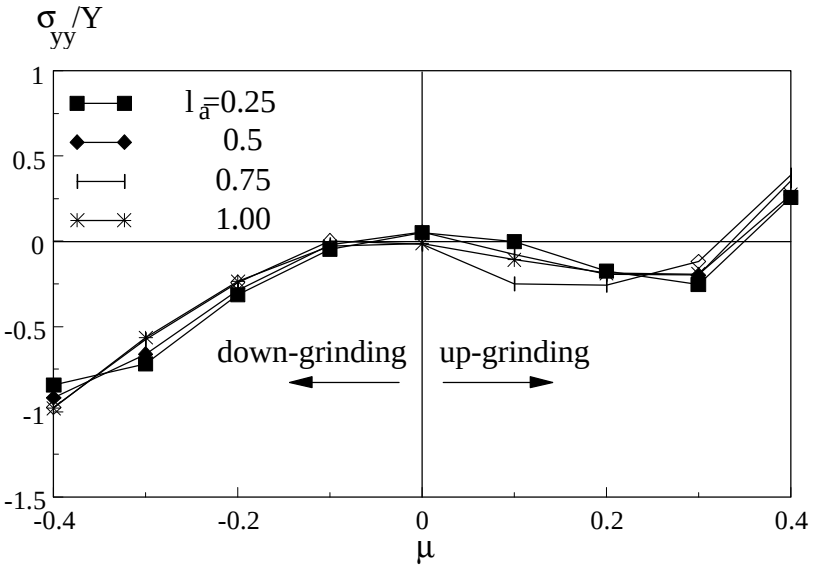

(b) σ_{yy}

Figure 5.7 Mechanical grinding surface residual ($p_a/Y=2.5$)

a continuous traction when the total grinding force, F_n, is the same.

significant influences on the magnitudes of the residual stresses under smaller active cutting area ratios. Thus the level and nature of grinding residual stresses are dominated by the sharpness of the active cutting grits particularly when the active to apparent area ratio is

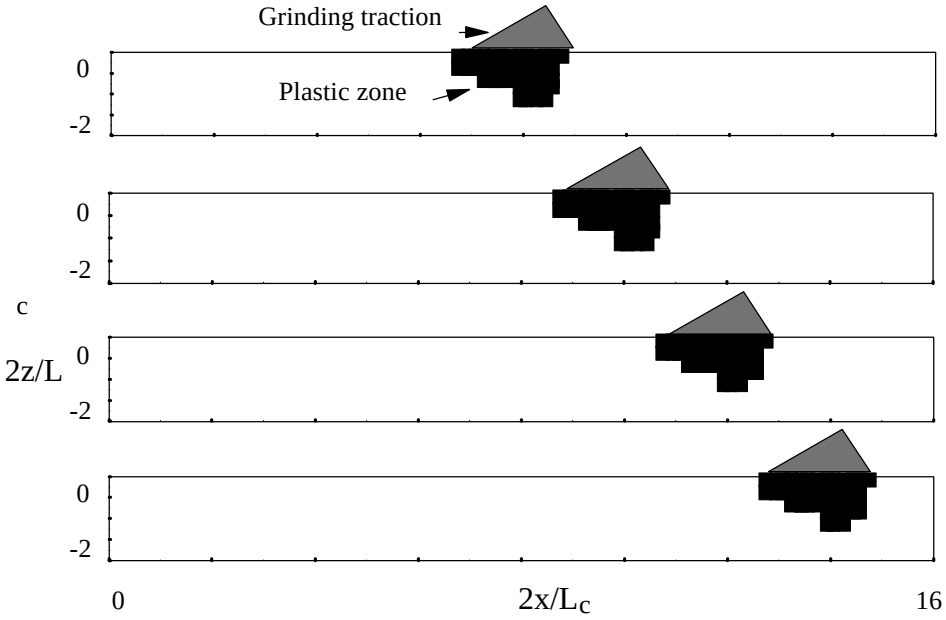

Figure 5.8 Plastic zone developments and mechanical movements (P_a=2.5 Y, μ=–0.4)

low. Practically, such a condition may be achieved using a grinding wheel with very sharp grits and fewer active cutting grits. An iso-thermal down-grinding mechanism of grinding is more advantageous than that of an up-grinding if residual stresses are involved. The results show that compressive stress can still be produced even if the active cutting area ratio is low. The iso-thermal up-grinding mechanism may result in compressive stresses for a number of limited cases. All the above indicates that the profile of interaction stresses between the grinding wheel and the workmaterial plays a significant role in determining the grinding-induced residual stresses.

5.3 Summary

In this chapter, the residual stresses due to iso-thermal mechanical grinding conditions were investigated. Section 5.1 considered the onset of mechanical iso-thermal plastic deformation in relation to a set of grinding conditions characterized by a wide range of traction profiles and ratios of tangential to normal traction. Section 5.2 demonstrated the resulting iso-thermal mechanical residual stresses in terms of grinding conditions.

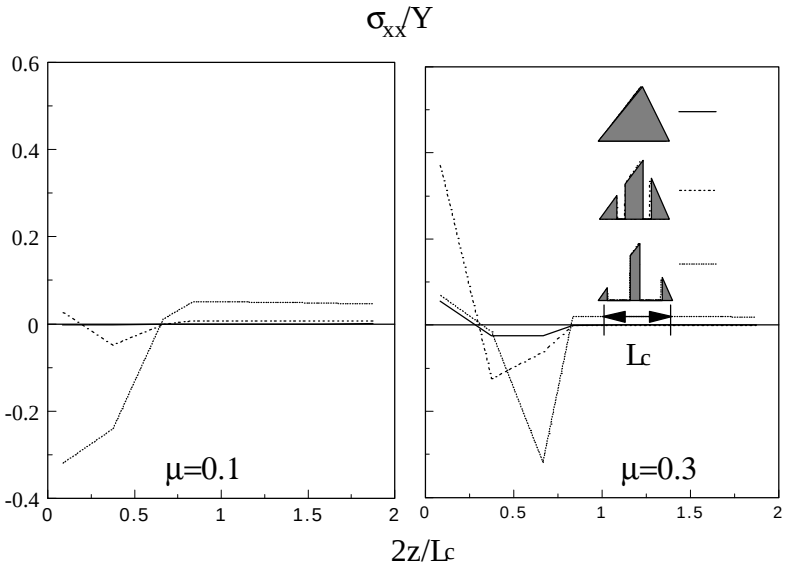

(a) σ_{xx},(l_a=0.25)

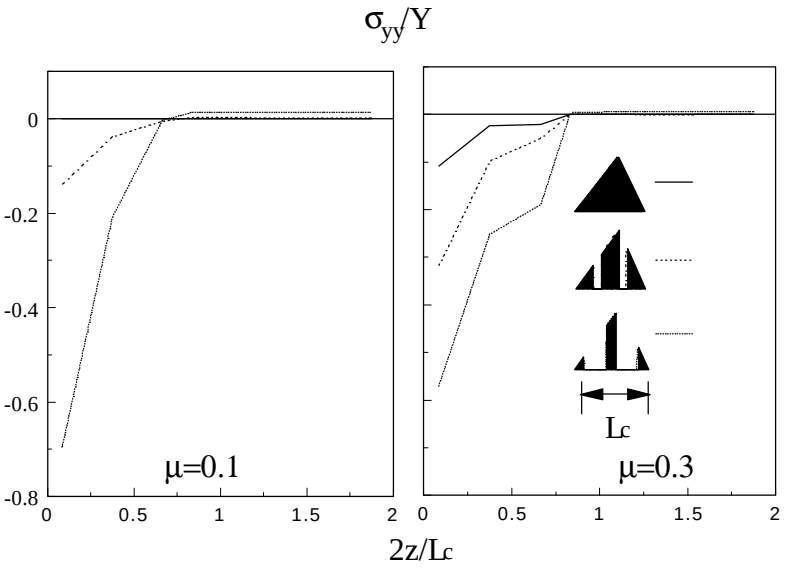

(b) σ_{yy},(l_a=0.25)

Figure 5.9 Mechanical grinding residual stresses, area ratio effect (Fn=1.875 Y L_c/2)

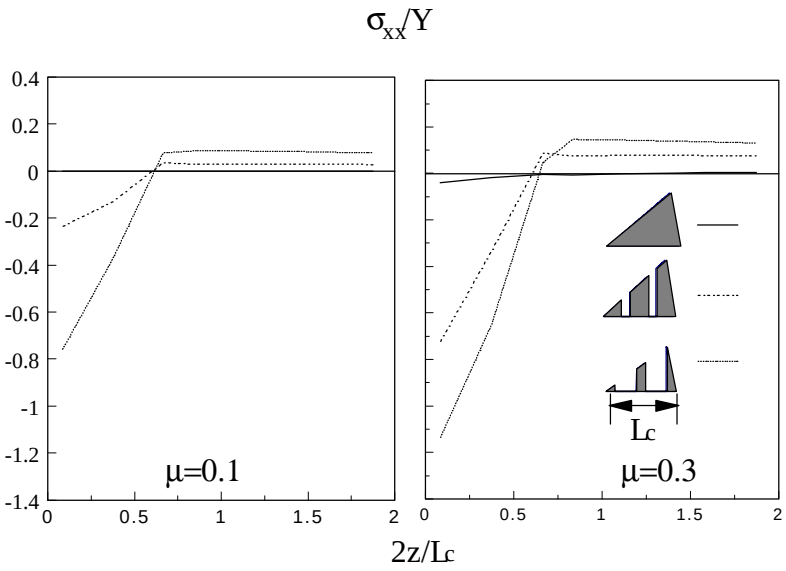

(c) σ_{xx},(l_a=0.75)

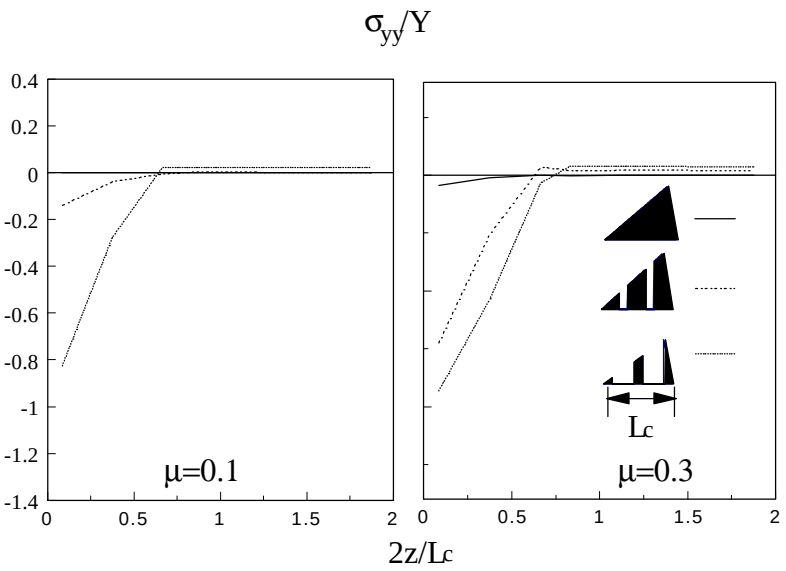

(d) σ_{yy},(l_a=0.75)

Figure 5.9 Mechanical grinding residual stresses, area ratio effect (Fn=1.875 Y L_c/2) (continued)